Electronic structure and properties of Ni-Si(001) and Ni-Si(111) reactive interfaces

O. Bisi,* L. W. Chiao,† and K. N. Tu
IBM Thomas J. Watson Research Center, Yorktown Heights, New York 10598
(Received 12 December 1983; revised manuscript received 15 June 1984)

A theoretical investigation of the Ni-Si(001) and Ni-Si(111) reactive interfaces using electronic band-structure calculation is presented. The following near-surface structures and interface models have been studied: (a) metastable adamantane structures of Ni interstitials in bulk Si at different stoichiometries: (b) isolated Ni interstitials near Si(001) and Si(111) surfaces; (c) single layer of $NiSi_2$ rotated by 180° on Si(111); and (d) Ni atom chemisorbed on a single layer of $NiSi_2$ on Si(111). The electronic properties of these structures and models are described and compared with the available experimental data. The low-Ni-coverage experimental results obtained for the (001) Si surface are interpreted in terms of an interfacial phase containing Ni interstitials in an adamantane geometry. For the (111) Si surface the experimental data provide evidence of both an interfacial phase containing Ni interstitials in an adamantane geometry and an epitaxial $NiSi_2$-Si(111) interface.

I. INTRODUCTION

Thin-film transition-metal silicides are of great current interest largely because of their application in electronic devices.[1,2] The formation of a silicide on Si depends on the metal/Si interfacial reaction. The Ni/Si interfaces are among the most reactive ones.[3–7] According to the proposed interstitial model,[8–11] the high reactivity of silicon surface upon near-noble metal deposition is due to the mobility of metal atoms. The metal atoms would move into the interstitial voids of the silicon lattice with very little activation energy and this would make the Si—Si bond less covalent and easier to break. Consequently, a low-temperature silicide formation can occur. Various surface techniques have been used to study submonolayer and monolayers of Ni deposited on well-characterized (111) and (001) Si surfaces and to characterize their electronic interaction and rearrangement of atomic positions. Among the findings are the following.

For the Si(111) surface, He light[12] and synchrotron radiation[13] photoemission spectroscopy shows a shift of the Ni d band towards the Fermi energy (E_F) upon increasing metal concentration. Epitaxial $NiSi_2$ film formed in an ultrahigh vacuum by a few monolayers of Ni deposited on Si(111) with subsequent annealing to ~450 °C, is found to be rotated by 180° with respect to the Si substrate (type-B orientation).[14–16] This observation is confirmed by a recent low-energy electron diffraction (LEED) study.[17] Surface-extended x-ray-absorption fine-structure (SEXAFS) measurements of Ni on Si(111) (Ref. 18) show a bond length of 2.37 Å and a sevenfold coordination number for the Ni atom. The SEXAFS results indicate that the Ni atoms must be located below the Si surface.

The as-deposited Ni on the Si(001) surface has been studied by x-ray photoelectron spectroscopy (XPS).[3] The interface is suggested to be a chemically graded region ranging from Si rich on the Si side to Ni rich on the Ni side. At the coverage of one monolayer (1 M.L.) the Ni $2p_{3/2}$ core level is found independent of the substrate temperature from 100 to 523 K. This supports a picture of Ni interstitials in the Si lattice.[10] Ion channeling experiment shows that a low-coverage Ni deposited on Si(001) at room temperature (RT) produces a dispersed Ni/Si interface, which could be explained by Ni occupying the interstitial voids in the Si lattice.[9] Ultraviolet photoemission spectroscopy (UPS), LEED, and transmission electron diffraction (TED) study of Ni on Si(001) with annealing, also lead to the suggestion of a diffusion layer of a distinctly metallic phase having $NiSi_2$ stoichiometry.[19,20] The diffusion-layer phase is formed by filling the octahedral interstitial voids of the Si lattice by Ni atoms,[19,20] leaving each metallic atom in an adamantane environment.[21]

We attempt to investigate the electronic structure of several different models of the Ni/Si interface or the near-surface structure upon depositing a few monolayers of Ni on both the (111) and (001) Si surfaces as deduced from the experimental results. The first is that of the adamantane structure. On varying the number of Ni interstitials, the stoichiometry of this metastable compound is varied from $NiSi_2$ to $NiSi_8$. The second model is that of the Ni interstitial in Si(001) and in Si(111). The third model is that of $NiSi_2$ epitaxial on Si(111), and the last is that of Ni atoms chemisorbed on one layer of $NiSi_2$ on Si(111). The calculations are to be compared with available experimental data.

II. METHOD OF CALCULATION

The theoretical method used for these complex models is the iterative extended Hückel theory (IEHT).[22] The approach is semiempirical and requires only the appropriate choice of the Slater orbital exponents and the Coulomb integrals, and a physically reasonable approximation to the exchange and resonance integrals. Iterations are made to achieve self-consistency in charge distribution on atoms. Using more sophisticated methods for these complex models would be computationally very difficult. The present semiempirical approach also extends easily from the bulk-structure calculation to surface- and interface-structure calculation and gives a consistent description of

both bulk and surface properties.[22–25,11]

The valence electron orbitals in a free atom $\phi_\alpha(\vec{r})$ are expressed by

$$\phi_\alpha(\vec{r})=[C_1\chi_{n,\xi_1}(r)+C_2\chi_{n,\xi_2}(r)]Y_{l,m}(\theta,\phi)\ ,$$
$$\alpha=(n,l,m)\ , \quad (1)$$

where $\chi_{n,\xi}(r)$ are Slater-type orbitals with orbital exponent ξ:

$$\chi_{n,\xi}(r)=(2n!)^{-1/2}(2\xi)^{n+1/2}r^{n-1}e^{-\xi r}\ , \quad (2)$$

and $Y_{l,m}(\theta,\phi)$ are the spherical harmonics. A double ξ expansion is essential in order to obtain a good description of the metal d orbital[26] necessary for the fitting of the bulk Ni band structure.

For each valence atomic orbital ϕ_α of each of the M atoms in the unit cell, one sets up a Bloch orbital for the crystal, given by

$$\Phi_{\alpha,i}(\vec{k},\vec{r})=\frac{1}{\sqrt{N}}\sum_l e^{i\vec{k}\cdot\vec{R}_{li}}\phi_\alpha(\vec{r}-\vec{R}_{li})\ ,$$
$$i=1,2,\ldots,M\ , \quad (3)$$

where $\vec{R}_{li}$ is the position of the ith atom in the lth unit cell, and N is the number of cells in the crystal. The Bloch functions are used as the basis to form energy eigenfunctions, i.e.,

$$\Psi_n(\vec{k},\vec{r})=[B_n(\vec{k})]^{-1/2}\sum_{i,\alpha}c_{\alpha,i}(\vec{k},n)\Phi_{\alpha,i}(\vec{k},\vec{r})\ , \quad (4)$$

where

$$B_n(\vec{k})=\sum_{i,\alpha}\sum_{j,\beta}c^*_{\beta,j}(\vec{k},n)c_{\alpha,i}(\vec{k},n)S_{\beta,j;\alpha,i}(\vec{k}) \quad (5)$$

is the normalization factor and

$$S_{\beta,j;\alpha,i}(\vec{k})=\frac{1}{N}\sum_{l,m}e^{i\vec{k}\cdot(\vec{R}_{li}-\vec{R}_{mj})}$$
$$\times\langle\phi_\beta(\vec{r}-\vec{R}_{mj})\,|\,\phi_\alpha(\vec{r}-\vec{R}_{li})\rangle \quad (6)$$

is the overlap matrix in the reciprocal space. The summation over unit cells l and m are taken over a finite number of shells. We found that for an interatomic distance greater than 7 Å the overlap contribution to the summation in (6) can be neglected.

The coefficients $c_{\alpha,i}(\vec{k},n)$ of the energy eigenfunction expansion (4) and the energy eigenvalues $E_n(\vec{k})$ are obtained by solving the secular equation

$$|H_{\beta,j;\alpha,i}(\vec{k})-E_n(\vec{k})S_{\beta,j;\alpha,i}(\vec{k})|=0\ , \quad (7)$$

where the matrix elements of the Hamiltonian H are

$$H_{\beta,j;\alpha,i}(\vec{k})=\frac{1}{N}\sum_{l,m}e^{i\vec{k}\cdot(\vec{R}_{li}-\vec{R}_{mj})}$$
$$\times\langle\phi_\beta(\vec{r}-\vec{R}_{mj})\,|\,H\,|\,\phi_\alpha(\vec{r}-\vec{R}_{li})\rangle\ . \quad (8)$$

In the extended-Hückel-theory (EHT) approximation the Coulomb integral $\langle\phi_\alpha(\vec{r}-\vec{R}_{li})\,|\,H\,|\,\phi_\alpha(\vec{r}-\vec{R}_{li})\rangle$ is set equal to the negative of the valence-orbital ionization potential (VOIP) (Ref. 27) of the corresponding atomic orbital $I_{\alpha i}$ and the resonance integrals are approximated by the expression:

$$\langle\phi_\beta(\vec{r}-\vec{R}_{mj})\,|\,H\,|\,\phi_\alpha(\vec{r}-\vec{R}_{li})\rangle$$
$$=-K_{\alpha\beta}\frac{I_{\alpha i}+I_{\beta j}}{2}\langle\phi_\beta(\vec{r}-\vec{R}_{mj})\,|\,\phi_\alpha(\vec{r}-\vec{R}_{li})\rangle\ . \quad (9)$$

The use of the arithmetic average of the ionization potential instead of the geometric average used in Ref. 22 for bulk silicides is necessary in order to adequately describe the conduction band of silicon, which is important for the present study. The iterative procedure is set up by allowing the $I_{\alpha,i}$'s to vary as a function of the excess charge on the atom itself q_i and of the excess charge on all the other atoms q_j:

$$I_{\alpha,i}(q_i,q_j)=I^0_{\alpha,i}+\mu_{\alpha,i}q_i+\sum_j\gamma_{ij}q_j\ , \quad (10)$$

where $I^0_{\alpha,i}$ is the ionization potential of the atomic orbital ϕ_α of the neutral atom at site i; μ and γ are intra-atomic and interatomic contributions per unit charge, respectively. Details of computation of these coefficients are given in the Appendix. At every iteration, the ionization potentials are varied according to the excess charges obtained from the previous iteration. The new values of $I_{\alpha,i}$ are used to calculate new excess charges, the procedure being repeated until convergence in the excess charge is achieved. The calculation was considered converged when the maximum deviation between input and output excess charges was less then 0.05 electrons/atom.

Charge transfer is not uniquely defined in a crystal compound, due to the arbitrariness of the bonding charge assignment to a specific atomic site. Reasonable and widely used prescriptions for defining the charge transfer are the Mulliken population analysis[28] and the Löwdin projection technique.[29] In the Mulliken approach the overlap charge between each pair of atom i and j of the unit cell is equally shared:

$$q^{\rm ov}_{\alpha,i}=2\sum_{j\,(\neq i)}\sum_\beta\sum_{\vec{k},n}[B_n(\vec{k})]^{-1}\int_{-\infty}^{E_F}dE\,c^*_{\beta,j}(\vec{k},n)S_{\beta,j;\alpha,i}(\vec{k})c_{\alpha,i}(\vec{k},n)\delta(E-E_n(\vec{k}))\ , \quad (11)$$

where $q^{\rm ov}_{\alpha,i}$ indicates the overlap contribution of the atomic orbital ϕ_α to the charge of the ith atom. The factor of 2 in Eq. (11) is due to spin degeneracy.

The Mulliken equal sharing of the overlap charge is believed to be justified when the bonds are far from ionicity, i.e., when the electronegativity difference between the different atoms is small.

The charge sitting on the ith atom is obtained by summing over all the ϕ_α's centered on that particular atom:

$$q_i=\sum_\alpha q_{\alpha,i}=\sum_\alpha q^A_{\alpha,i}+q^{\rm ov}_{\alpha,i}\ , \tag{12}$$

where

$$q^A_{\alpha,i}=2\sum_\beta \sum_{\vec{k},n}[B_n(\vec{k})]^{-1}\int_{-\infty}^{E_F} dE\, c^*_{\beta,i}(\vec{k},n)S_{\beta,i;\alpha,i}(\vec{k})c_{\alpha,i}(\vec{k},n)\delta(E-E_n(\vec{k})) \tag{13}$$

is the net atomic contribution of the orbital ϕ_α to the charge of the ith atom.

In the Löwdin approach the nonorthogonal atomic orbitals ϕ_α are transformed to the orthogonal wave functions $\tilde{\phi}_\alpha$. In the transformed orthogonal basis set the energy eigenfunctions are

$$\Psi_n(\vec{k},\vec{r})=\sum_{i,\alpha}\tilde{c}_{\alpha,i}(\vec{k},n)\tilde{\Phi}_{\alpha,i}(\vec{k},\vec{r})\ , \tag{14}$$

where $\tilde{\Phi}_{\alpha,i}$ is the Block superposition of the orthogonal orbital $\tilde{\phi}_\alpha(\vec{r}-\vec{R}_{li})$ [see Eq. (3)]. In the Löwdin population analysis the contribution of the atomic orbital ϕ_α to the charge of the ith atom is given by

$$q_{\alpha,i}=2\sum_{\vec{k},n}\int_{-\infty}^{E_F} dE\,|\tilde{c}_{\alpha,i}(\vec{k},n)|^2\delta(E-E_n(\vec{k}))\ . \tag{15}$$

The approximation arises from the fact that the orthogonal basis-set Bloch function $\tilde{\Phi}_{\alpha,i}$ is a combination of different orbitals and sites contributions:

$$\tilde{\Phi}_{\alpha,i}(\vec{k},\vec{r})=[B_n(\vec{k})]^{-1/2}\sum_{\beta,j}\Phi_{\beta,j}(\vec{k},\vec{r})S^{-1/2}_{\beta,j;\alpha,i}(\vec{k})\ . \tag{16}$$

We set up the iterative procedure of Eq. (10) using both prescriptions for the charge-transfer evaluation. In $NiSi_2$ both calculations converge at similar charges and densities of states (DOS), with a difference in the Ni charge of 0.11 electrons/atom. This shows that it is possible to define a meaningful charge transfer for the Si-Ni compounds. All the calculations we present here are based on a Mulliken population analysis.

The atomic wave function Slater exponents, as well as the Si and Ni orbital-dependent parameters $K_{\alpha\beta}$ of Eq. (9) have been adjusted to reproduce the electronic band of pure Si and Ni as suggested by Messmer *et al.*[30] The parameters used for calculation are listed in Table I. The values of $K_{\alpha\beta}$ for the Si-Ni s-p interaction are taken as the average between the corresponding $K_{\alpha\beta}$ parameters for Si and Ni. For the s-d and p-d interaction the $K_{\alpha\beta}$ parameters are assumed to be the same as the pure Ni Hamiltonian. All the models we study in the present work are investigated using these input data by varying the geometric structure, with no free parameters. The interface calculation has been performed by solving the secular equation of a slab of 16 (001) or 12 (111) Si layers containing four or three Si atoms per layer, respectively.[31,32]

TABLE I. Input parameters for Si and Ni.

	Si		Ni		
Orbital	$3s$	$3p$	$4s$	$4p$	$3d$
C_1	1.00	1.00	0.485	1.00	0.421
ξ_1 (a.u.$^{-1}$)	1.90	1.43	3.12	2.20	5.03
C_2			0.608		0.706
ξ_2 (a.u.$^{-1}$)			1.71		2.15
$I_{\alpha,i}$ (eV)	14.95	7.77	6.80	3.11	7.69
$\mu_{\alpha,i}$ (eV)	12.39	10.13	7.95	5.75	12.57
$K_{\alpha\alpha}$		1.75		2.5	
$K_{\alpha\beta}$		1.46		2.5	

Figure 1 shows the Si energy band as computed using the data of Table I. We found a valence bandwidth of 12.91 eV and an indirect gap along the ΓX direction of 1.19 eV, in good agreement with the results of more sophisticated calculations.[33]

III. RESULTS

The DOS for bulk $NiSi_2$ together with the Ni and Si contribution is shown in Fig. 2 as a reference for the analysis of the models to be investigated. The interaction between Si p and Ni d states leads to a partial dehybridization of the Si s states near -10 eV, the sp^3 configuration of Si being changed toward s^2p^2. This effect, which is fully accomplished in a metal-richer stoichiometry,[22,34] is responsible here for the presence of the p-d bonding-antibonding structures straddling the main d peak at -5.6 and -2.0 eV, respectively. The energy position of the d-band main peak at -3.3 eV is in good agreement with other theoretical calculations[35,36] and experimental data.[24]

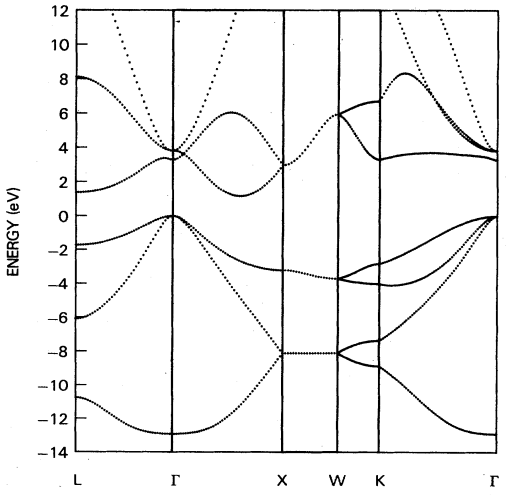

FIG. 1. Si energy bands computed with the parameters of Table I.

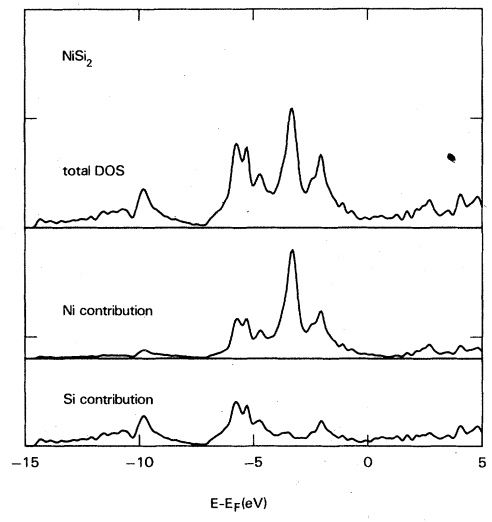

FIG. 2. Theoretical DOS and partial density of states for bulk $NiSi_2$.

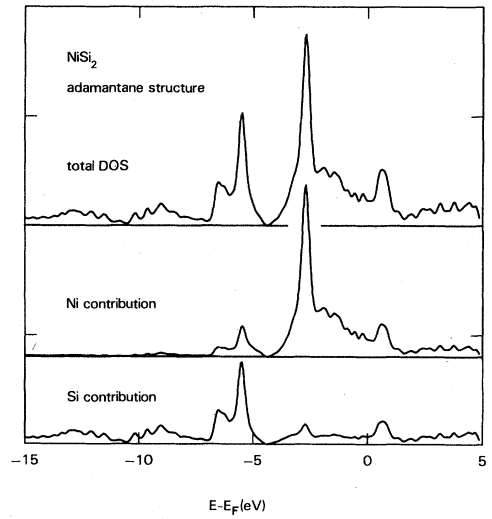

FIG. 4. Theoretical DOS and partial density of states for $NiSi_2$ adamantane structure.

A. Adamantane structure

The Ni interstitial adamantane geometry has been proposed in order to interpret ion-channeling,[9] UPS, and TED experiments.[19,20]

In this structure a Ni atom lies in a ten-atom cage of undistorted Si atoms which consists of two subsets of atoms (Fig. 3): a set of four (*A* atoms, shaded circles) that lie at the vertices of a tetrahedron and a set of six (*B* atoms, circles of unbroken perimeter) that lie at the vertices of an octahedron. The distance between centers of the interstitial (solid circle) and the *A* and *B* atoms is 2.35 and 2.71 Å, respectively. By varying the number of occupied adamantane sites by Ni in the Si, we vary the stoichiometry of this compound from $NiSi_2$ to $NiSi_8$. In regard to the adamantane structure of $NiSi_2$, we note that this cubic compound does not correspond to a stable crystal structure, but has been proposed as a diffusion layer structure[20] at the interface between silicon and nickel. The undistorted Si (adamantane structure of $NiSi_2$) lattice volume is greater than that of stable $NiSi_2$, which has the same crystal structure as CaF_2, by 1.3%. While in the CaF_2 structure every Ni atom has eight Si neighbors at a distance of 2.34 Å, in the adamantane $NiSi_2$ the Ni atoms have only four Si atoms at 2.35 Å, the other six being at 2.71 Å. The weaker Si-Ni interaction leads to a reduction of the number of states involved in the Si—Ni bond. Because of this reduction the *d* band is shifted towards lower binding energies (BE) as we may expect from the fact that this compound is unstable. The main *d* peak is

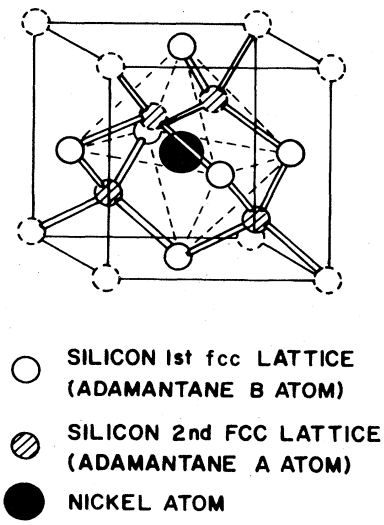

FIG. 3. The adamantane structure of the Si cages inside a Si crystal. The six face-centered Si atoms of the first lattice form the octahedron cage. The four second-lattice Si atoms form the tetrahedral cage.

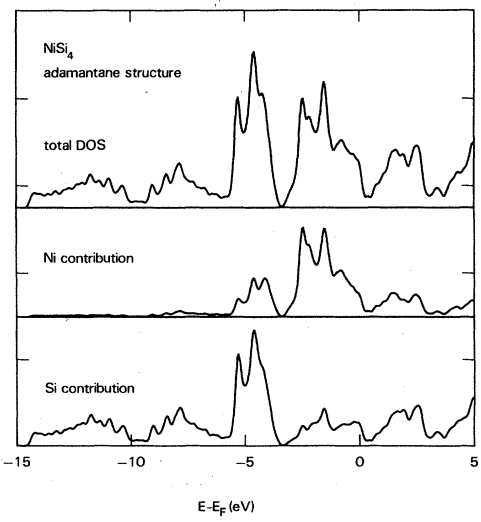

FIG. 5. Theoretical DOS and partial density of states for $NiSi_4$ adamantane structure.

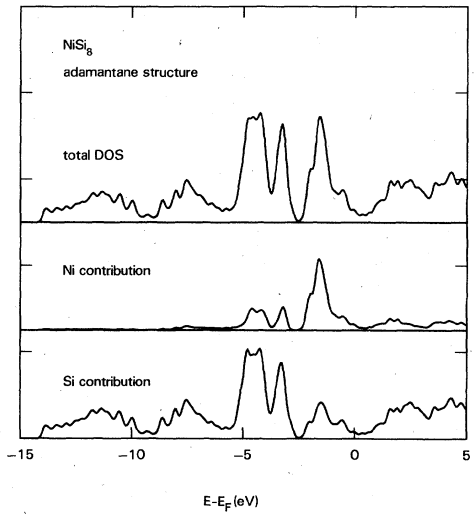

FIG. 6. Theoretical DOS and partial density of states for $NiSi_8$ adamantane structure.

sharp and lies at −2.7 eV (Fig. 4).

In the adamantane structure of $NiSi_4$ and $NiSi_8$ the local coordination of every Ni atom does not change from that of the adamantane structure with $NiSi_2$ stoichiometry. On going towards the more Si-rich phases, the Si DOS approaches the Si-bulk tetrahedral features, showing corresponding changes in the interaction of Si with the Ni atoms.

The nonbonding *d* states are found in the energy region corresponding to the Si bulk gap (Figs. 5 and 6). In $NiSi_4$ these states form a peak with a 2-eV width centered at −2.0 eV; in $NiSi_8$ this peak is found at −1.6 eV. The trend of peak shift found in these interstitial adamantane Si-rich phases is the opposite of the trend found in the Si-Ni stable compounds, where a shift of the *d* band towards higher BE has been found on going towards Si-rich stoichiometry.[24] The DOS features of $NiSi_4$ and $NiSi_8$ in an undistorted Si lattice cannot be understood in terms of a Si-Ni chemical interaction, which leads to a compound formation that minimizes the total energy. The energy of the Ni *d* states in the adamantane structure is constant if it is referred to the vacuum level and it lies in the same energy range as the Si bulk gap. On increasing Ni content the Fermi energy is shifted towards lower BE so that the relative position of the Ni *d* band moves in the opposite direction.

B. Ni interstitial in Si surface layer

In order to explain the high reactivity of Si surfaces upon near-noble-metal deposition, an interstitial mechanism has been proposed.[8–11] From this point of view the silicide formation occurs because of the weakening of the Si—Si bonds by the interstitial metals. For the interstitial mechanism to be effective in weakening bonds of the Si surface atoms, we have to study the effect of Ni interstitials immediate below the surface. Both Si(001) and Si(111) surfaces are considered in the following. Figure 7 shows a cross-sectional view of the interstitial geometry

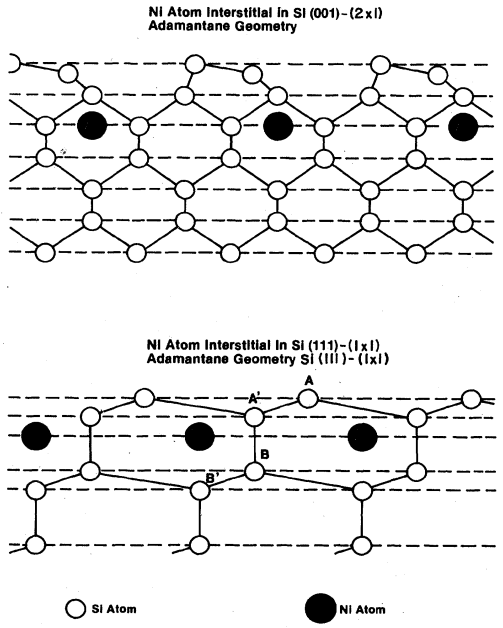

FIG. 7. Geometries for Ni interstitial in Si(001) and in Si(111).

studied for the Si(001). The clean surface Si atoms form a 2×1 reconstructed lattice. Several models have been proposed in order to account for this reconstruction; none has reached a complete description of the experimental data.[37] Among them the asymmetric-dimer model[31] gives a good description of the electronic properties of the surface, and it is simple enough to permit an interstitial interface calculation. The interstitial metal atom in the early stages of deposition does not bond significantly with the Si surface atoms, so that we may suppose that the Si clean-surface reconstruction is unchanged. In the following we will show that the results for Ni interstitial below a reconstructed Si(001) and an ideal Si(111) surface are similar. This provides evidence that the Si-Ni interaction does not depend significantly upon the status and orientation of the Si surface. We therefore followed this model and simulated the Si(001) surface with a slab of 16 Si(001) layers (20.4 Å thick).

In order to have information on the very early stages of the Ni deposition, we have to study the Ni in the limit of diluted impurity. We chose a two-dimensional (2D) square unit cell of 7.68 Å size (four Si atoms per 2D cell). Ni atoms lie in a 2D periodic square array of the same size as shown in Fig. 7 and their mutual interaction is negligible. The projected densities of states (PDOS) for the Ni atom and for the two Si atoms, which in an undistorted surface lie along the [001] direction directly on the top and below the interstitial site, are shown in Fig. 8. The reconstruction increases the Si_{up}Ni distance from 2.71 to 2.79. The interaction between Ni and Si neighbors leads to several features in the density of states.

While the interaction with the Si_{up} atom is responsible for the contribution of *d* peak around E_F, the bonding with the interior Si atoms (including the Si_{down} atom) leads to a sharp peak at −3.8 eV. Figure 8 shows also a

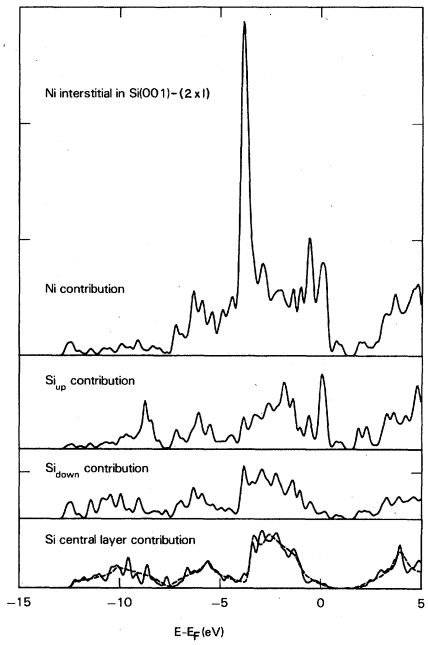

FIG. 8. Theoretical partial density of states for Ni interstitial in Si(001)-(2×1). Si_{up} (Si_{down}) atom lies on the [001] direction on the top (directly below) the interstitial Ni. Lower panel dash curve shows the Si bulk DOS.

comparison between the Si central layer PDOS and the Si bulk density of states indicating that the number of (001) layers was sufficient to avoid interactions between the two surfaces of the slab. For the reasons mentioned above we limit our present study to an undistorted Si(111)-(1×1) surface. A cross-sectional view of the geometry of the Ni interstitial in the Si(111) model is shown in Fig. 7.

It is useful to compare the PDOS found in the $NiSi_8$ adamantane structure (Fig. 6) with the PDOS of the Ni interstitial in Si(111) (Fig. 9). In both models an isolated

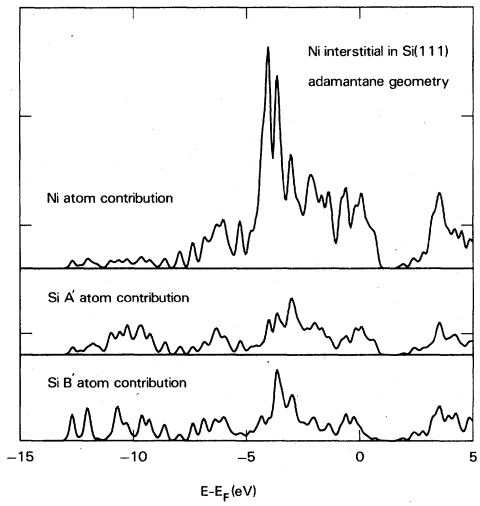

FIG. 9. Theoretical partial density of states for Ni interstitial in Si(111). Si A' (Si B') atom indicates Ni first neighbor of the A' (B') Si(111) plane (see Fig. 7).

Ni atom lies in an adamantane cage. In $NiSi_8$ the bulk Si atoms interact weakly with the impurity atom, leaving the Ni d state in a nonbonding configuration. In the case of an interstitial Ni atom below a Si(111) surface we found a considerable increase of the number of Si—Ni bonding states, leading to a shift of the main d peak to −3.9 eV below E_F. This effect, which has already been found in the Pd/Si(111) system,[11] is due to the greater reactivity of the Si surface atoms, being no longer in a bulk sp^3 configuration. The earlier results found in the Si(001)-(2×1) surface show that there the reconstruction has a weaker effect.

C. $NiSi_2$ epitaxial layer on Si(111)

The Si(111) surface constitutes a 2D hexagonal lattice of atoms at a distance of 3.84 Å, while the hexagonal array of a $NiSi_2$(111) layer are at a distance of 3.82 Å. It is this close lattice match that makes the growth of a uniform epitaxial film of $NiSi_2$ on Si(111) possible.[14] However, when the film is very thin, the lattice of $NiSi_2$ has been found rotated by 180° about the normal to the Si surface.[15–17] Figure 10 shows the two ways a $NiSi_2$ layer may be matched to a Si(111) substrate. In both models (A geometry and B geometry) the $NiSi_2$ layer is rotated by 180°. In the A geometry the Ni atom lies in a substitutional site with seven Si neighbors at 2.35 Å, to be compared with the eight Si neighbors at 2.34 Å in the $NiSi_2$ bulk. The Si atom below the $NiSi_2$ layer lies in the ideal surface adamantane voids; it is surrounded by three Ni at 2.35 Å and six Si atoms at 2.71 Å. The silicon atoms in this $NiSi_2$ interface layer are strongly perturbed with respect to both the $NiSi_2$ and Si bulk densities of states (Fig. 11). The Si-Ni interaction leads to a structured d band, with two distinct peaks at −4.1 and −4.9 eV.

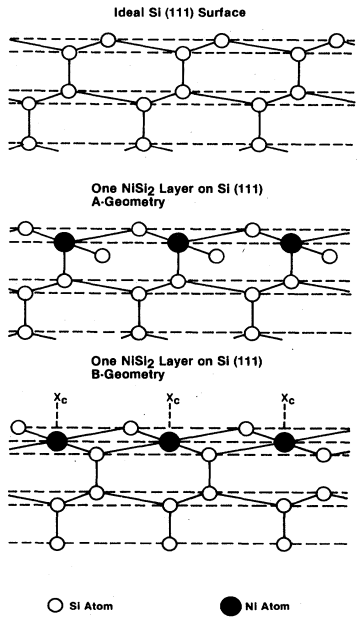

FIG. 10. Geometry of the Si(111) clean surface and of one $NiSi_2$ layer on Si(111) in the A and B geometry. x_c indicates the Ni chemisorption site.

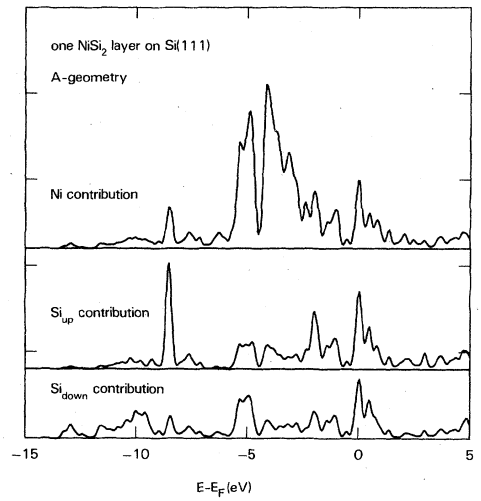

FIG. 11. Theoretical partial density of states for one $NiSi_2$ layer on Si(111) A geometry. Si_{up} (Si_{down}) refers to the upper (lower) $NiSi_2$ single-layer Si atom.

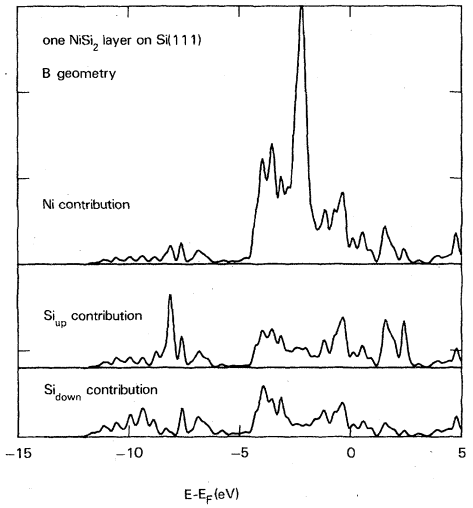

FIG. 13. Theoretical partial density of states for one $NiSi_2$ layer on Si(111) B geometry. Si_{up} (Si_{down}) refers to the upper (lower) $NiSi_2$ single-layer Si atom.

In the B geometry the Ni atoms lie in a six- Si-atom coordination site, at the same distance of 2.35 Å as in the A geometry. With respect to the former interface geometry, in this case the lowering of the coordination number leads to a weaker Si-Ni intersection. At the lower binding energy site of the Si—Ni bonding peak we have an essentially nonbonding structure. This sharp peak is located at 2.2 eV below E_F.

D. Ni chemisorbed on one layer of $NiSi_2$ on Si(111)

We study also a model of Ni-enriched surface of the $NiSi_2$/Si(111) interface. Our model is set up by putting a Ni atom on top of the Ni atom in $NiSi_2$ (x_c site of Fig. 10).

In this way we obtain sevenfold coordination number for the B geometry too, but in a Ni-richer environment than in the A geometry. Figure 12 shows the PDOS for this last case. The Ni d states are clearly grouped in three distinct peaks. It is instructive to compare these results with the $NiSi_2$ layer on the Si(111) case of the same B geometry (Fig. 13). The Ni—Si bonding peak at higher BE is still present, while the Ni peak at −2.2 eV is broadened by the Ni-Ni interactions. A new sharp structure, characteristic of the chemisorbed Ni atom, is found at 0.9 eV below E_F.

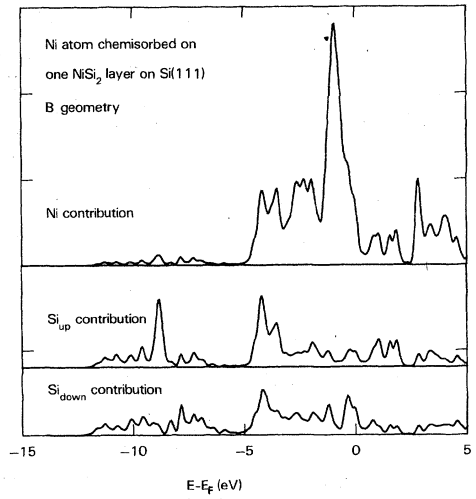

FIG. 12. Theoretical partial density of states for a Ni atom chemisorbed on one $NiSi_2$ layer on Si(111) B geometry. Si_{up} (Si_{down}) refers to the upper (lower) $NiSi_2$ single-layer Si atom.

IV. DISCUSSION

The aim of the present work is to investigate the mechanism of the Si-Ni interaction following Ni deposition onto clean Si(001) and Si(111) surfaces. Figure 14 shows a summary of the results for the different models we have studied. We plot the Ni $3d$ contribution because we are mainly interested in a comparison with photoemission data [Refs. 3, 19, and 20 for Ni/Si(001) and Refs. 12 and 13 for Ni/Si(111) interfaces] with a dominant Ni $3d$ photoionization cross section.

It is important to note that these calculations have been performed without any free parameter except the geometry of the crystal structures investigated, so the different locations of the Ni d band reflect the different geometric configurations.

In the top panel the results for bulk Ni_2Si, NiSi, and $NiSi_2$ show the narrowing of the Ni d band and the shift of the main Ni d peak towards higher BE on increasing Si concentration. The good agreement between these calculations and the experimental data[24] encourages us to extend the analysis to interfacial problems.

A. Ni on Si(001) surface

The evaporation of Ni onto Si(001) followed by annealing produces TED superlattice spots characteristic of an ordered structure of Ni and Si. The structure could be identified as the stable $NiSi_2$ (CaF_2) or adamantane structure of $NiSi_2$ on the basis of the geometry of the diffrac-

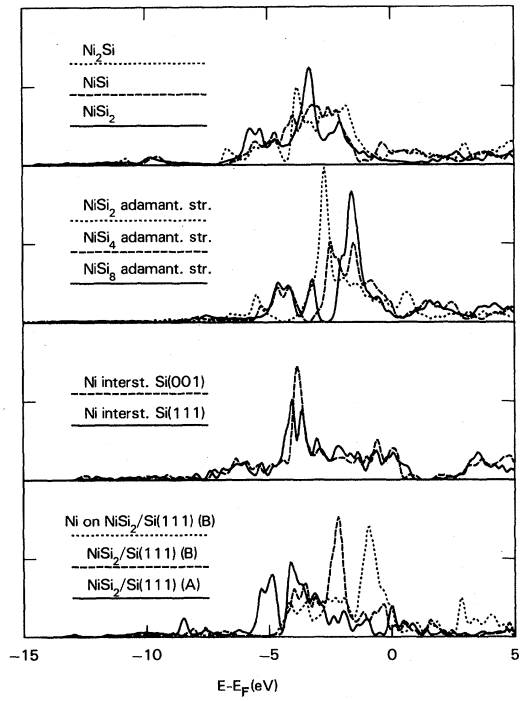

FIG. 14. Summary of the theoretical Ni partial density of states for bulk silicides and for the interface models considered in the present study. The normalization is to the number of electron per Ni atom.

tion pattern.

Photoemission spectroscopy exhibits a peak at 2.78 eV below E_F which could be attributed to Ni atoms diffused into a Si lattice.[20] This peak at −2.78 eV is to be compared with the bulk silicides characteristic features at −3.2, −1.8, and −1.3 eV for $NiSi_2$, NiSi, and Ni_2Si, respectively.[12,20,24] Our results show that on going from the bulk $NiSi_2$ to the adamantane structure of $NiSi_2$, a shift of the main d peak from −3.3 to −2.7 eV takes place. The correct prediction of the energy position of the d band on going from bulk compound to interdiffusion layer strongly supports the picture of Ni interstitial diffusion at the interface, with the formation of a $NiSi_2$ adamantane structure rather than the stable $NiSi_2$ compound having the CaF_2 structure.

A second structure, seen in photoemission at very low coverage, at 1.9 eV below E_F, has been attributed to a surface chemisorbed species of Ni.[20] We do not find a unique way to interpret this peak. The chemisorbed site assignment indicates a surface Ni enrichment at the beginning of the deposition. On varying the chemisorption site and/or the Si—Ni bond length it is possible to find a d-band peak fitting the experimental value.

A different explanation of the −1.9-eV peak may be found in the emission from Ni atoms in a $NiSi_8$ adamantane environment. A deconvolution of the two experimental peaks (see Fig. 7 of Ref. 20) may shift the smaller one towards E_F, leading to a better agreement with our $NiSi_8$ result (1.6 eV below E_F). If this is the correct interpretation, it indicates that the interdiffusion of Ni in Si at very low coverages produces regions of different stoichiometries. The UPS signal detection from Ni atoms in the interdiffusion layer at submonolayer coverage may be due to the migration of isolated Ni atoms towards compound-formation regions, leading to an initial inhomogeneous formation.

A third explanation may be found if the interdiffusion-layer compound is both homogeneous and without surface-Ni enrichment. In this case both the structures found at −2.78 and −1.9 eV can be interpreted as arising from Ni atoms in $NiSi_4$ adamantane structure.

Our results can also interpret an unexplained, up to now, XPS experimental result. Grunthaner *et al.*[10] found a coincidence of the Ni $2p_{3/2}$ BE at 0.3—1 M.L. of Ni on Si(001) with that of the stable NiSi compound. Since each Ni atom in NiSi is surrounded by six Si and four Ni atoms, it seems unlikely that the NiSi coordination environment could exist at such low coverage.

We can qualitatively explain this result by using the approach of Franciosi *et al.*[38] interpreting the BE shift of silicides by different stoichiometries. On the basis of this approach the variations in the silicide core-level BE are mainly due to the effect of changing electronic configuration rather than relaxation and charge transfer. On increasing Si concentration the Ni configuration moves towards an atomic configuration $3d^8 4s^2$ and the core level shifts towards higher BE.[39]

Our results (Table II) show that the Ni d electron configuration in an adamantane $NiSi_2$ is intermediate between NiSi and bulk $NiSi_2$. If the core-level BE is mainly determined by the electronic configuration we expect the interdiffusion-layer core level to be intermediate between NiSi and $NiSi_2$.

The effect of the charge transfer is to shift the core-level BE of all bulk silicides in the same direction. Therefore, we may infer a similar core-level BE for Ni in both $NiSi_2$ adamantane structure and NiSi compound.

The interpretation of the UPS data in terms of bulk interdiffusion compounds instead of subsurface interstitials (third panel of Fig. 14) means that the interstitial diffusion is not limited to the Si surface layer. The ~12-Å electron escape depth of the UPS experiment investigates

TABLE II. Ni d electron configuration and total charge transfer.

	Ni d configuration	Excess charge (e/at.)
Ni_2Si	8.82	−0.04
NiSi	8.70	−0.10
$NiSi_2$ (adamantane structure)	8.50	+0.06
$NiSi_2$ CaF_2	8.20	−0.12

a region of ~9 Si(001) layers, and the diffusion layer has to be at least of this order of magnitude.

B. Ni on Si(111) surfaces

This interface has been recently studied with different techniques, with particular interest in the $NiSi_2$-Si epitaxial growth.[14–18]

A room-temperature precursor-surface-layer compound formed by interdiffusion has been proposed.[16] The formation of epitaxial $NiSi_2$ has been detected after heating this layer at 450 °C. On the other hand, if unreacted Ni is present on top of this surface-layer compound it will instead transform to Ni_2Si and NiSi upon annealing.[16]

Room-temperature SEXAFS analysis of Ni on Si(111) shows that the short-range environment surrounding Ni atoms is similar (although not identical) to that encountered in a $NiSi_2$ lattice,[18] the main difference being a sevenfold coordination number rather than the eightfold for Ni in $NiSi_2$.

Ni deposition on Si(111) followed by annealing at high temperature (900—1200 °C) produces two different phases, depending on the Ni coverage.[17] The LEED analysis of the high-coverage phase confirms a $NiSi_2$ epitaxial layer, rotated by 180° with respect to the Si substrate. In the low-coverage case a LEED 1×1 phase, similar to the quenched "1×1" clean Si(111) surface is found.

UPS experiments on Ni deposited on Si(111) show that intermixing between Si and Ni occurs at very low temperature (85 K).[12] The room-temperature spectra, shifted by 0.1—0.6 eV towards higher BE, show a greater dispersion of Ni into the Si lattice. At a coverage of 1.5 M.L. a broad d band is bound at −1.85 eV (−1.95 at RT). On increasing metal coverage there is a continuous d-band shift towards E_F.

Room-temperature synchrotron radiation experiments[13] show very similar data. A difference spectrum at submonolayer coverage shows a broad d peak at −1.8 eV [full width at half maximum (FWHM), ~2 eV].

Among the various models we studied, only the $NiSi_4$ adamantane structure and the B-geometry interface between one layer of $NiSi_2$ and Si(111) produce a d band centered around 2 eV below E_F (Fig. 14). The shape of these peaks is different: In the $NiSi_4$ case a wide peak (FWHM of 2 eV), asymmetric in the low BE site, occurs, while in the second model of $NiSi_2$ a 2.5-eV-wide band, with a very narrow peak (FWHM of 0.6 eV) at −2.2 eV is found. On the basis of the available experimental data it is difficult to discriminate between these two models. Photoemission line shape[12,13] is closer to the PDOS of the $NiSi_4$ model, while SEXAFS (Ref. 18) data provided evidence of formation of $NiSi_2$/Si(111) B-geometry interface at coverages as low as 0.5 M.L.

The results found in the low-coverage Ni/Si(111) interface cannot be directly compared with the low-coverage Ni/Si(001) interface. While Si(111) data has been taken at 85 K and room temperature, the Si(001) experiment has been performed after annealing at 473 K and 703 K.

In the 4—6 M.L. coverage room-temperature photoemission shows a d-band peak at −1.40 eV (4 M.L.) and −0.95 eV (6 M.L.). The result can be interpreted in terms of the Ni chemisorbed on the $NiSi_2$/Si(111) model. This agreement is due to the low coordination of the chemisorbed Ni atom, directly bonded to a single Ni atom. If we could increase the chemisorbed Ni interactions by increasing the coordination number we would obtain a shift to higher BE of the d peak.

From the above discussion, we see that while a great deal of experimental work on the Ni/Si interfaces has been performed, it is not possible to piece them together to achieve a firm understanding of the interface because of the lack of a systematic approach. The key issue is how to correlate atomic position and rearrangement with chemical or electronic interaction on a Si surface upon Ni deposition. We should be able to gain a better picture by starting the experiment at a very low temperature so that the deposited Ni atoms will be chemisorbed on a clean Si surface without moving into the Si layer, and then by performing combined measurements using diffraction techniques such as LEED and spectroscopic techniques such as UPS in a multitechnique chamber, or by the use of a transfer device without breaking the ultra-high vacuum to monitor the interaction as a function of annealing temperature. The result will no doubt offer a better insight to the interfacial reaction and in turn to the construction of theoretical models.

V. CONCLUSIONS

We have investigated the electronic properties of different models of Ni/Si(001) and Ni/Si(111) interfaces. Our results, showing the modification of the chemical bond and of the electronic properties caused by stoichiometry or geometrical variations, are a useful tool to interpret the experimental information of these interfaces.

Our analysis of the available experimental data gives evidence of the existence of both interfacial phases containing Ni interstitials in an adamantane geometry and silicide-silicon epitaxial interface. At present the relation between these different Ni configurations and the dynamics of the probable transition between them is not well understood.

ACKNOWLEDGMENTS

We are extremely grateful to P.M. Marcus (International Business Machines Corporation), F. Comin (Bell Telephone Laboratories Incorporated), and A. Franciosi (University of Minnesota) for stimulating discussions.

APPENDIX

The ionization potential of the neutral atom $I^0_{\alpha,i}$ and the intra-atomic charge contribution $\mu_{\alpha,i}$ are determined through the valence-orbital ionization potentials of the free atom (VOIP's).[40] The VOIP for a transition $M_a^q \rightarrow M_b^{q+1}$ corresponding to the ionization of an electron from the configuration M_a to form the configuration M_b is given by

$$V_{\rm IP}^{\rm VO}(q)=I_a(q)+E(M_b)-E(M_a)\ , \tag{A1}$$

where q is the excess charge on the atom, $I_a(q)$ is the ground-state ionization potential of M_a^q, and $E(M_b)$ and $E(M_a)$ are the average energies of the two configurations, obtained from the weighted mean of the energies of all the multiplet terms. The VOIP values of Table I have been determined by using spectroscopic data[41] and the Slater-Condon parameters to evaluate the average energies of multiplets[42,43] for neutral atom M_a^0 and positive ion M_a^{+1} initial configuration. The intra-atomic charge contribution $\mu_{\alpha,i}$ determined through a positive-ion configuration is used for both positive and negative excess charge on the atom.

The interatomic contribution to the ionization potential depends on the values of the electron repulsion integrals:

$$I(\vec{R}_{li},\vec{R}_{hj},\vec{R}_{mt},\vec{R}_{nu})=\langle\phi_\alpha(\vec{r}_1-\vec{R}_{li})\phi_\alpha(\vec{r}_2-\vec{R}_{hj})\,|\,C\,|\,\phi_\beta(\vec{r}_1-\vec{R}_{mt})\phi_\delta(\vec{r}_2-\vec{R}_{nu})\rangle\ , \tag{A2}$$

where $C=|\vec{r}_1-\vec{r}_2|^{-1}$ is the Coulomb potential and $\phi_\alpha(\vec{r}-\vec{R}_{li})$ is the atomic valence orbital of the ith atom in the lth unit cell. Rather than calculate the many center repulsion integrals, we approximate them with a spherically averaged Coulomb repulsion integral:

$$I(\vec{R}_{li}-\vec{R}_{hj})=\langle\phi_s(\vec{r}_1-\vec{R}_{li})\phi_s(\vec{r}_2-\vec{R}_{hj})\,|\,C\,|\,\phi_s(\vec{r}_1-\vec{R}_{li})\phi_s(\vec{r}_2-\vec{R}_{hj})\rangle\ . \tag{A3}$$

Despite the great simplification in the numerical calculation, this averaging has only a slight effect on the electron energies.[44,45]

The spherically averaged repulsion integral behaves asymptotically as an electrostatic point-charge potential and is screened at shorter range. In the spirit of our semiempirical approach we computed the values of $I(\vec{R}_{li}-\vec{R}_{hj})$ through the Ohno-Klopman approximation:[46]

$$I(\vec{R}_{li}-\vec{R}_{hj})=\left[(\vec{R}_{li}-\vec{R}_{hj})^2+\frac{1}{4}\left[\frac{1}{\Gamma_i}+\frac{1}{\Gamma_j}\right]^2\right]^{-1/2}\ . \tag{A4}$$

The formula is written in atomic units and Γ_i is set equal to the difference between the ionization potential and electron affinity of the ith atom.[47] The Ohno-Klopman formula is a good approximation to the electron repulsion integral in the internuclear distance range that we are interested in (greater than 2 Å).[48]

The interatomic contribution to the ionization potential of the ith atom is

$$\sum_j\left[\sum_h{}'I(\vec{R}_{li}-\vec{R}_{hj})\right]q_j=\sum_j\gamma_{ij}q_j\ . \tag{A5}$$

The prime on the summation excludes the $h=0$ term when $i=j$. The lattice summation in large parentheses may be performed in reciprocal space using the Ewald technique. The spherically averaged repulsion integral [Eqs. (A3) and (A4)] is screened near the origin so that there is no problem of convergence at large reciprocal vectors. Formulas for lattice summation for both three-dimensional (bulk silicides) and 2D lattices (slab geometry) may be found in Appendix B of Ref. 49.

*Permanent address: Institute of Physics, University of Modena, I-41100 Modena, Italy.

†Permanent address: Department of Physics, Georgetown University, Washington, D.C. 20057.

[1]K. N. Tu and J. W. Mayer, in *Thin Films—Interdiffusion and Interactions,* edited by J. M. Poate, K. N. Tu, and J. W. Mayer (Wiley, New York, 1978), p. 359.

[2]G. Ottaviani, J. Vac. Sci. Technol. **16**, 1112 (1979).

[3]P. J. Grunthaner, F. J. Grunthaner, and J. W. Mayer, J. Vac. Sci. Technol. **17**, 924 (1980).

[4]I. Abbati, L. Braicovich, U. del Pennino, B. De Michelis, and S. Valeri, Le Vide, les Couches Minces **201**, 959 (1980) [Proceedings of the Fourth International Conference on Solid Surfaces (ICSS-4) and the Third European Conference on Surface Science (ECOSS-3) Cannes, France, 22—27 September 1980].

[5]G. W. Rubloff, P. S. Ho, J. F. Freouf, and J. E. Lewis, Phys. Rev. B **23**, 4183 (1981).

[6]G. W. Rubloff and P. S. Ho, Thin Solid Films, **93**, 21 (1982).

[7]N. W. Cheung, R. J. Culbertson, L. C. Feldman, P. J. Silverman, K. W. West, and J. W. Mayer, Phys. Rev. Lett. **45**, 120 (1980).

[8]K. N. Tu, Appl. Phys. Lett. **27**, 221 (1975).

[9]N. W. Cheung and J. W. Mayer, Phys. Rev. Lett. **46**, 671 (1981).

[10]P. J. Grunthaner, F. J. Grunthaner, A. Madhukar, and J. W. Mayer, J. Vac. Sci. Technol. **19**, 649 (1981).

[11]O. Bisi and K. N. Tu, Phys. Rev. Lett. **52**, 1633 (1984).

[12]I. Abbati, L. Braicovich, B. De Michelis, U. del Pennino, and S. Valeri, Solid State Commun. **43**, 199 (1982).

[13]K. L. I. Kobayashi, S. Sugaki, A. Ishizaka, Y. Shiraki, H. Daimon, and Y. Murata, Phys. Rev. B **25**, 1377 (1982).

[14]K. C. R. Chin, J. M. Poate, J. E. Rowe, T. T. Sheng, and A. G. Cullis, Appl. Phys. Lett. **38**, 988 (1981).

[15]D. Cherns, G. R. Anstis, J. L. Hutchison, and J. C. H. Spence, Philos. Mag. A **46**, 849 (1982).

[16]R. T. Tung, J. M. Gibson, and J. M. Poate, Phys. Rev. Lett. **50**, 429 (1983).

[17]W. S. Yang, F. Jona, and P. M. Marcus, Phys. Rev. B **28**, 7377 (1983).

[18]F. Comin, J. E. Rowe, and P. H. Citrin, Phys. Rev. Lett. **51**, 2402 (1983).

[19]Y. J. Chang and J. L. Erskine, Phys. Rev. B **26**, 4766 (1982).

[20]Y. J. Chang and J. L. Erskine, Phys. Rev. B **28**, 5766 (1983).

[21]F. A. Cotton and G. Wilkinson, *Advanced Inorganic Chemistry* (Wiley, New York, 1980), p. 59.

[22]O. Bisi and C. Calandra, J. Phys. C **14**, 5479 (1981).

[23]O. Bisi and L. W. Chiao, Phys. Rev. B **25**, 4943 (1981).
[24]A. Franciosi, J. H. Weaver, D. G. O'Neill, Y. Chabal, J. E. Rowe, J. M. Poate, O. Bisi, and C. Calandra, J. Vac. Sci. Technol. **21**, 624 (1982).
[25]O. Bisi, C. Calandra, L. Braicovich, I. Abbati, G. Rossi, I. Lindau, and W. E. Spicer, J. Phys. C **15**, 4707 (1982).
[26]J. W. Richardson, W. C. Nieuwpoort, R. R. Powell, and W. F. Edgell, J. Chem. Phys. **36**, 1057 (1962).
[27]H. Basch, A. Viste, and H. B. Gray, J. Chem. Phys. **44**, 10 (1966).
[28]R. S. Mulliken, J. Chem. Phys. **23**, 1833 (1955).
[29]P. O. Löwdin, J. Chem. Phys. **18**, 365 (1950).
[30]R. P. Messmer, S. K. Knudson, K. H. Johnson, J. B. Diamond, and C. Y. Yang, Phys. Rev. B **13**, 1396 (1976).
[31]D. J. Chadi, Phys. Rev. Lett. **43**, 43 (1979).
[32]K. C. Pandey and J. C. Phillips, Phys. Rev. Lett. **32**, 1433 (1974).
[33]J. R. Chelikowsky and M. L. Cohen, Phys. Rev. B **14**, 556 (1976).
[34]P. S. Ho, G. W. Rubloff, J. E. Lewis, V. L. Moruzzi, and A. R. Williams, Phys. Rev. B **22**, 4784 (1980).
[35]Y. J. Chabal, D. R. Hamann, J. E. Rowe, and M. Schlüter, Phys. Rev. B **25**, 7598 (1982).
[36]D. M. Bylander, L. Kleinman, K. Mednick, and W. R. Grise, Phys. Rev. B **26**, 6379 (1982).
[37]D. E. Eastman, J. Vac. Sci. Technol. **17**, 492 (1980), and references therein.
[38]A. Franciosi, J. H. Weaver, and F. A. Schmidt, Phys. Rev. B **26**, 546 (1982).
[39]A. R. Williams and N. D. Lang, Phys. Rev. Lett. **40**, 954 (1978).
[40]H. Basch, A. Viste, and H. B. Gray, J. Chem. Phys. **44**, 10 (1966).
[41]C. E. Morre, *Atomic Energy Levels,* National Bureau of Standards, (U.S.A.) (U.S. G.P.O., Washington, D.C., 1958).
[42]J. C. Slater, *Quantum Theory of Atomic Structure* (McGraw-Hill, New York, 1960).
[43]J. Hinze and H. H. Jaffe, J. Chem. Phys. **38**, 1834 (1963).
[44]A. Breeze, P. M. Magee, and P. G. Perkins, J. Non-Cryst. Solids **13**, 140 (1973).
[45]A. Zunger, Phys. Rev. B **17**, 626 (1977).
[46]K. Ohno, Theor. Chim. Acta **2**, 219 (1964); G. Klopman, J. Am. Chem. Soc. **86**, 4550 (1964).
[47]H. B. Micaelson, IBM J. Res. Dev. **22**, 72 (1978).
[48]B. Dick and G. Hohlneicher, Theor. Chim. Acta **53**, 221 (1979).
[49]M. P. Tosi, in *Solid State Physics,* edited by F. Seitz and D. Turnbull (Academic, New York, 1964), Vol. 16.